Stem Cells Translational Medicine, 2022, **11**, 539–551
https://doi.org/10.1093/stcltm/szac009
Advance access publication 23 March 2022
Original Research

Neural Stem Cell-Derived Exosomal Netrin1 Contributes to Neuron Differentiation of Mesenchymal Stem Cells in Therapy of Spinal Bifida Aperta

Ling Ma[1,2], Xiaowei Wei[1], Wei Ma[1], Yusi Liu[1], Yanfu Wang[1], Yiwen He[1], Shanshan Jia[1], Yu Wang[1,3], Wenting Luo[1], Dan Liu[1], Tianchu Huang[1], Jiayu Yan[2], Hui Gu[1], Yuzuo Bai[1], Zhengwei Yuan[1,*]

[1]Key laboratory of Health Ministry for Congenital Malformation, Department of Pediatric Surgery, Shengjing Hospital, China Medical University, Shenyang, Liaoning, People's Republic of China
[2]Department of Pathophysiology, College of Basic Medical Science, China Medical University, Shenyang, Liaoning, People's Republic of China
[3]Department of Ultrasound, Shengjing Hospital, China Medical University, Shenyang, Liaoning, People's Republic of China

*Corresponding author: Zhengwei Yuan, Key laboratory of Health Ministry for Congenital Malformation, Department of Pediatric Surgery, Shengjing Hospital, China Medical University, No. 36, Sanhao Street, Heping District, Shenyang 110004, China. Tel: +86 24 23929903; Email: yuanzw@hotmail.com

Abstract

Spinal bifida aperta (SBA) is a congenital malformation with a high incidence. Bone marrow mesenchymal stem cell (BMSC) transplantation has the potential to repair the structure of damaged tissues and restore their functions. This is an optional treatment that can be used as a supplement to surgery in the treatment of SBA. However, the application of BMSCs is limited, as the neuronal differentiation rate of BMSCs is not satisfactory when used in treating severe SBA. Thus, we aimed to assess the effect of neural stem cell (NSC)-derived exosomes on BMSC neuronal differentiation and observe the therapeutic effect in an ex vivo rat SBA embryo model. We found that NSC-derived exosomes increased the neuronal differentiation rate of BMSCs in vitro and in the SBA embryo model ex vivo. Proteomic analysis showed that NSC-derived exosomes were enriched in Netrin1, which positively regulated neuronal differentiation. Netrin1 increased the neuronal differentiation rate of BMSCs and NSCs and upregulated the expression of the neuronal markers, microtubule-associated protein (Map2), neurofilament, and β3-tubulin. Bioinformatic analysis revealed that Netrin1 treatment increased the expression of the transcription factors Hand2 and Phox2b, related to neuronal differentiation. Furthermore, the Netrin1-induced NSC neuronal differentiation was significantly blocked by Phox2b knockdown. We suggest that NSC-derived exosomal Netrin1 induces neuronal differentiation via the Hand2/Phox2b axis by upregulating the expression of Hand2 and Phox2b. Therefore, NSC-derived exosomes are a critical inducer of BMSC neuronal differentiation and represent a potential treatment agent that can benefit BMSC treatment in SBA.

Key words: spinal bifida aperta; exosomes; neural stem cell; bone marrow mesenchymal stem cells; neuron differentiation; Netrin1

Graphical Abstract

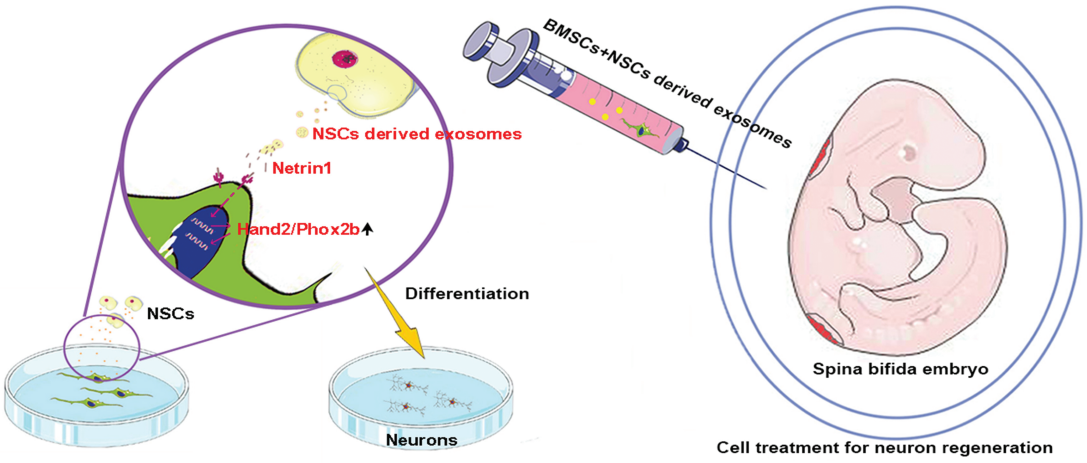

Received: 3 August 2021; Accepted: 24 January 2022.

Introduction

Spinal bifida aperta (SBA) is the failure of neural tube closure along the dorsal spine and occurs in 2 to 6 per 10 000 live births worldwide.[1,2] Despite advancements in surgical repair of fetal SBA, a significant portion of neonates undergoing in utero repair still experience neurological, lower motor neuron, and urinary/gastrointestinal morbidity.[3,4] Therefore, it is necessary to develop new therapeutic alternatives that can repair neuronal damage and complement surgery shortcomings.

Cell therapy is an attractive therapeutic option that can achieve structural and functional regeneration after tissue damage due to any cause, using cell replacement.[5] Among the various types of cell therapies, stem cell therapy has emerged as an effective therapeutic approach for SBA. Neural stem cells (NSCs) are undoubtedly the preferred stem cell source for the treatment of neural injury. However, their utilization is limited primarily owing to host immune rejection, as the transplanted cells are not autologous. Bone marrow mesenchymal stem cells (BMSCs) are one of the most frequently studied adult stem cell types owing to the broad range of cell types that they are able to generate, their low immunogenicity, ease of collection and availability for auto-transplantation at any stage of life and, importantly, their low tumorigenicity risk.[6-8] Many studies on the potential use of MSCs for the treatment of neural tube defects (NTDs) have demonstrated that transplanted MSCs could reverse neurological damages in various SBA animal models.[9-20] However, the application of BMSCs is limited, as their neural differentiation rate is not satisfactory when used in treating severe SBA.

MSCs and NSCs exert positive effects on each other when co-cultured.[21] BMSCs are able to generate neural stem-like cells under NSC induction.[22] Furthermore, cell therapies using co-transplantation of MSCs and NSCs in various neurological disease models, such as spinal cord or brain injury, Parkinson's disease, and Alzheimer's disease, have been reported.[23,24] Recently, it has been shown that exosomes can be released by nearly all cell types and participate in various physiological or pathological processes such as tissue repair and antigen presentation.

Exosomes have attracted attention as important mediators of intercellular communication. Furthermore, exosomes offer considerable advantages, such as a high safety profile and low immunogenicity, over NSCs. Hence, the use of exosomes can overcome many of the risks and challenges associated with cell therapy, especially immune rejection. Cell-specific proteins, lipids, and nucleic acids in exosomes can act as signaling molecules that can be transmitted to other cells to modulate their function. Thus, we speculated that NSCs induce neuronal MSC differentiation through NSC-derived exosomes encapsulating specific NSC-derived molecules that can sustain the neural phenotype.

Thus, we hypothesized that NSC-derived exosomes could be used to improve neuronal differentiation of BMSCs in cell therapy of SBA, which has not been previously reported. We also aimed to reveal the mechanism underlying NSC-induced BMSC neuronal differentiation.

Materials and Methods

Animals

Wistar rats were obtained from the animal center of China Medical University. Female virgin rats, 10-12 weeks old, were mated with healthy males of the same strain. Pregnancy was confirmed the following morning by the presence of sperm in the vaginal smear, and this was considered as day 0 of gestation. All experimental procedures involving animals were approved by the ethics committee of China Medical University (2020PS372K(X1)).

Cell Culture

Rat primary BMSCs, rat primary hippocampus-derived NSCs, and mouse NSC lines were used in this study. BMSCs were isolated from rat bone marrow. The method used for BMSC isolation, identification, and culture has been previously described.[13,14] NSCs were isolated from rat hippocampus. Briefly, rat hippocampi, dissected from E14 embryos, was mechanically disassociated by gentle pipetting. Primary cells were grown to allow formation of neurospheres. For immune-staining of neurospheres, the floating spheres were hydrogel-embedded (ShakeGelTM3D, Hangzhou Kevin Biotechnology Co., Ltd, China) and then processed in a way similar to the processing of adherent cells. NSCs were identified using Nestin immunostaining. The culture supernatant of NSCs was harvested for exosome purification.

Exosome Purification, Characterization, and Analysis

Exosomes were purified using sequential centrifugation. The cell culture supernatant of NSCs was harvested and spun at 300 × *g*, 4 °C for 20 minutes and 2000 × *g*, 4 °C for 20 minutes, successively. Then, the supernatant was filtered using a 0.22-μm filter, and then, spun at 10 000 × *g*, 4 °C for 1 hours. Finally, exosomes were collected following spinning at 100 000 × *g*, 4 °C for 4 hours. Exosomes were washed in phosphate-buffered saline (PBS) and pelleted again using ultracentrifugation. The purified exosome pellet was resuspended in PBS. Exosomes were verified, using transmission electron microscopy (TEM) (80 Kv, 60 000×, H-7650, HITACHI, Japan). The exosome size and particle number were analyzed using a Laser Particle Size and Zeta Potential Analyzer (Nano ZS90, Malvern Instruments, UK), and expression of the exosome protein markers Alix and CD9 was analyzed using Western blotting.

Exosome Tracer Assay

Rat primary NSCs were stained with both Dio Cell-Labeling Solution (V22886, Life Tech, USA) and SYTO Red Fluorescent Nucleic Acid Stain (S34900, Life Tech) according to the manufacturer's instructions. Exosomes isolated from the Dio- and SYTO-stained NSCs were labeled simultaneously. BMSCs were cultured in medium supplemented with labeled exosomes for 24 hours. Next, BMSCs were washed twice with PBS, fixed in 4% paraformaldehyde, and stained with DAPI. Fluorescence signals of exosomes were captured using a confocal microscope.

Neuronal Differentiation Conditions

Neuronal differentiation of BMSCs was induced using NSC-derived exosomes. BMSCs (10^4 cells/well) were cultivated in medium supplemented with 100 μg/mL NSC-derived exosomes, while BMSCs without exosomes were used as the control. Cells were allowed to differentiate for 7 days.

Neuronal differentiation of BMSCs was induced using recombinant Netrin1 (rNetrin1). BMSCs (10^4 cells/well)

were cultivated in medium supplemented with 500 ng/mL rNetrin1, while BMSCs cultured without rNetrin1 were used as the control. Cells were allowed to differentiate for 12 days.

rNetrin1 was also used to induce neuronal differentiation in a mouse NSC line. NSCs (10^3 cells/well) were cultivated in medium supplemented with 500 ng/mL rNetrin1, while mouse NSCs cultured without rNetrin were used as the control. Cells were allowed to differentiate for 7 days.

Whole-Embryo Culture

Dams were sacrificed on the morning of gestation day 10. The decidua was dissected from the uteruses. Only embryos having an intact visceral yolk sac, ectoplacental cone, and amnion, were placed in culture medium, which was normal rat serum containing 2 mg/mL glucose. To induce SBA, atRA (Sigma-Aldrich) was added to the culture medium at a concentration of 10 μM. As developmental stage variation at the start of culture could affect the in vitro development, embryo selection was performed. Embryos with 8-12 somites, 2 or 3 brain vesicles, and S-shaped tubular heart were selected. BMSCs, combined with or without NSC-derived exosomes, were injected into the amniotic cavity of the embryos with a glass micropipette connected to a Hamilton syringe. For BMSC visualization after transplantation into the rat fetus, BMSCs were transfected with an enhanced green fluorescent protein (GFP) adeno-5 expression vector. Four embryos each were placed in a presterilized culture bottle containing 3 mL culture medium. Culture bottles were placed in a roller apparatus and rotated at 30 rpm in a 37 °C incubator with a continuous supplement of a gas mixture, including different concentrations of oxygen (5% O_2 for the first 18 hours, 20% O_2 from 19 to 36 hours, and 60% O_2 from 37 to 48 hours). The embryos were checked for survival, indicated by the presence of a yolk sac circulation and heartbeat. The embryos were harvested at 48 hours and fixed with 4% paraformaldehyde for 24 hours, followed by dehydration in 20% sucrose for 24 hours. Then, they were sectioned into 20 μm serial transverse sections, and all GFP-positive BMSCs in the spinal column were observed. Sections with GFP-positive BMSCs were kept at −80 °C for further immunofluorescence analyses.[25]

Proteomic Analysis

For sample preparation, protein was extracted using SDT buffer and quantified. A total of 20 μg protein/sample was separated using 12.5% sodium dodecyl sulfate-polyacrylamide gel electrophoresis (SDS-PAGE). Protein bands were visualized using Coomassie Blue R-250 staining.

For protein filter-aided sample preparation and digestion, 200 μg of protein/sample was added to 30 μL SDT buffer (4% SDS, 100 mM DTT, 150 mM Tris-HCl, pH 8.0). After the detergent, DTT and other low-molecular-weight components were removed and reduced cysteine residues were blocked, the protein suspensions were digested with 4 μg trypsin (Promega) in 40 μL 25 mM NH_4HCO_3 buffer, and the resulting peptides were collected. Then, the peptides were desalted on C18 Cartridges (Emproe SPE Cartridges C18 [standard density], bed ID 7 mm, volume 3 mL, Sigma), concentrated using vacuum centrifugation, and reconstituted in 40 μL of 0.1% (v/v) formic acid. The OD_{280} of the resulting peptides was measured.

For label-free liquid chromatography with tandem mass spectrometry (LC-MS/MS), each fraction was injected for nano LC-MS/MS analysis. The peptide mixture was loaded onto a reverse phase trap column (Thermo Scientific Acclaim PepMap100, 100 μm × 2 cm, nanoViper C18) connected to a C18-reversed phase analytical column (Thermo Scientific Easy Column, 10 cm long, 75 μm inner diameter, 3 μm resin) in buffer A (0.1% formic acid) and buffer B (84% acetonitrile and 0.1% formic acid) at a flow rate of 300 nL/minute. The 120 minutes LC gradient was 0%-55% buffer B for 110 minutes, 55%-100% buffer B for 5 minutes, held in 100% buffer B for 5 minutes.

MS data were acquired using a data-dependent top 10 method dynamically selecting the most abundant precursor ions from the survey scan (300-1800 *m/z*) for higher energy collisional dissociation (HCD) fragmentation. The automatic gain control target was set to 3 and 6, and the maximum injection time to 10 ms. The dynamic exclusion duration was 40.0 s. Survey scans were acquired at a resolution of 70 000 at *m/z* 200, whereas the resolution for HCD spectra was set to 17 500 at *m/z* 200, and the isolation width was 2 *m/z*. The normalized collision energy was 30 eV and the under-fill ratio was defined as 0.15. The instrument was run with peptide recognition mode enabled. The MS data were analyzed using MaxQuant software version1.5.3.17 (Max Planck Institute of Biochemistry in Martinsried, Germany).

Bioinformatic Data Mining

We searched for Netrin1 in the Gene Expression Omnibus (GEO) database of NCBI and obtained the GSE54107 dataset. This dataset contains RNA sequencing data (Illumina HiSeq 2000, Mus musculus) of mouse fibroblasts ($n = 2$) and mouse fibroblasts grown in media supplemented with rNetrin1 ($n = 4$). The expression matrix file was downloaded.

Bioinformatic Analysis

Differentially expressed proteins were analyzed to identify significantly down- or upregulated proteins according to the criteria of fold difference >2 and $P < .05$. A heat map was presented as a visual aid of protein relative expression data. The Database for Annotation, Visualization and Integrated Discovery (DAVID) was used to conduct Gene Ontology (GO) analysis. The GO standard was used to categorize proteins according to 3 ontologies, namely, biological process (BP), molecular function (MF), and cellular component (CC). GO enrichment was applied based on the Fisher' exact test. Benjamini-Hochberg correction for multiple testing was further applied to adjust the derived *P*-values. Only functional categories with *P*-values < .05 were considered statistically significant. The heat map and GO annotation results were plotted using R scripts. The protein–protein interaction (PPI) information of the studied proteins was retrieved using the STRING software. The results were downloaded in the XGMML format and imported into the Cytoscape5 software to visualize and further analyze the functional PPI networks.

Immunostaining

Whole-embryo sections were analyzed by immunofluorescence staining using rabbit anti-β3-tubulin (#5568, Cell Signaling Technology, USA, a neuronal marker), rabbit anti-synapsin-1 (#5297S, Cell Signaling Technology, USA, a synaptic marker), and mouse anti-GFP antibody (ab1218, Abcam, USA) to label the transplanted MSCs. In brief, after antigen retrieval, sections were washed in PBS and then blocked with a blocking serum containing 0.1% Triton X-100 (v/v). Subsequently, sections were incubated with an anti-β3-tubulin

antibody (1:50) combined with an anti-GFP antibody (1:50) or anti-synapsin-1 antibody (1:50) combined with an anti-GFP antibody (1:50). Afterward, sections were washed in PBS followed by incubation with both an Alexa-conjugate goat anti-rabbit IgG (1:100, #4413, Cell Signaling Technology) and an Alexa Fluor 488-conjugated goat anti-mouse IgG (1:100, #4408, Cell Signaling Technology). After washing, cell nuclei were stained with 4, 6-diamidino-2-phenyl indole (DAPI). To determine the percentage of BMSC differentiation, all GFP-positive cells and GFP and β3-tubulin double-positive cells were counted. The neuronal differentiation rate of BMSCs was determined as the number of β3-tubulin and GFP double-positive cells/total number of GFP-positive cells, and the number of synapsin-1 and GFP double-positive cells/total number of GFP-positive cells.

The neuronal differentiation rate of BMSCs and NSCs was evaluated with immunocytochemical staining. Briefly, cells were fixed in 4% paraformaldehyde for 30 minutes, washed with PBS, and then blocked with blocking serum containing 0.1% Triton X-100 (v/v). Next, the cells were incubated with a β3-tubulin antibody and a TRITC-conjugate goat anti-rabbit IgG antibody (1:100). Cell nuclei were stained with DAPI and counted to estimate the number of total cells. The number of β3-tubulin-positive cells was counted. The neuronal differentiation rate was determined as the number of β3-tubulin-positive cells/total cell number.

Western Blot Analysis

Total protein extraction was performed using a radioimmunoprecipitation assay solution. Protein concentration was measured using the BCA assay, and an equal quantity of each sample (100 μg) was used for Western blotting. Following SDS-PAGE, the proteins were transferred onto 0.45 μm polyvinylidene difluoride membranes (IPVH00010, Millipore, USA). Membranes were blocked with 5% (w/v) non-fat dry milk in Tris base saline Tween 20 (TBST; 50 mM Tris, pH 8.0, 150 mM NaCl, and 0.1% Tween-20 (v/v)) for 1.5 hours, and then, washed thrice for 10 minutes in TBST, followed by incubation at 4 °C overnight with mouse anti-Alix (ab88743, Abcam), rabbit anti-CD9 (ab223052, Abcam), rabbit anti-Netrin1 (ab126729, Abcam), mouse anti-NF (#2836, Cell Signaling Technology), rabbit anti-microtubule-associated protein (MAP2) (#4542, Cell Signaling Technology), rabbit anti-β3-tubulin (#5568, Cell Signaling Technology), rabbit anti-Phox2b (25276-1-AP, Proteintech Group Inc, USA), rabbit anti-Hand2 (abs117611, Absin Bioscience Inc., China), GAPDH (10494-1-AP, Proteintech Group Inc), and Lamin A/C (ab169532, Abcam). Next, the membranes were washed thrice in TBST and incubated with a secondary antibody at room temperature for 2 hours. Following washing with TBST, the reaction was detected using chemiluminescence and the Western Bright ECL detection kit (WBKLS00100, USA).

shRNA Transfection

Mouse NSCs (1×10^3 cells/well) were seeded in 6-well plates. Phox2b shRNA experiments were performed using Hu6-MSC-CMV-GFP-SV40-Neomycin vectors and three siRNA targeted Phox2b sequences (shPhox2b, Genechem Co. Ltd., Shanghai, China), (shPhox2b-1 target sequence: 5′-GCGTCTTATCTTCGCTCCAAA-3′,shPhox2b-2targetsequence:5′-CGGCCTCAACGAGAAACGCAA-3′,shPhox2b-3 target sequence: 5′-CGCAGTTTAGACATCTCTGTT-3′). In parallel, an unrelated sequence was designed as a negative control (NC) for siRNA specificity. Plasmid transfection was performed using lipofectamine 3000 (L3000015, Invitrogen, USA).

Statistical Analysis

Statistical analyses were performed using the SPSS 22.0 software. Results are presented as the means ± standard error of mean of 3 independent experiments. Differences between 2 groups were analyzed using Student's *t* tests, whereas differences among multiple groups were analyzed using 1-way analysis of variance. A *P*-value of <.05 was considered to indicate statistical significance.

Results

Generation and Initial Characterization of NSCs and NSC-Derived Exosomes

Primary NSCs from the rat hippocampus were observed to proliferate, form neurospheres floating in the culture medium (Supplementary Fig. S1A), and express NSC markers (Supplementary Fig. S1B). NSC exosomes were isolated from the NSC culture medium; TEM (Supplementary Fig. S2A) and dynamic light scattering analyses (Supplementary Fig. S2B) revealed that the particles isolated using ultracentrifugation, most of which had diameters of approximately 80 nm, contained abundant exosomes, as evidenced by expression of the exosomal protein markers Alix and CD9 in these fractions (Supplementary Fig. S2C).

NSC-Derived Exosomes Promoted BMSC Neuronal Differentiation In Vitro and In Vivo

To trace NSC-derived exosomes, an exosome tracer assay was performed (Fig. 1A). NSCs were stained with the Dio green fluorescent dye, which binds to cell membranes, and the SYTO red fluorescent dye, which binds to nucleic acids. The exosomes derived from the stained NSCs were simultaneously labeled with Dio and SYTO. After the labeled exosomes were added into the culture medium of BMSCs for 24 h, green and red fluorescence signals were also detected in the BMSCs (Fig. 1A), indicating that the NSC-derived exosomes had been taken up by the BMSCs.

To investigate the effect of NSC-derived exosomes on BMSC neuronal differentiation, BMSCs were treated with NSC-derived exosomes for 2, 5, and 7 days. As the duration of culture with NSC-derived exosome supplement increased, more BMSCs showed neuron-like morphological changes (Fig. 1B). Consistent with the observed neuron-like morphological changes, immunofluorescence staining revealed a high efficiency of differentiation by day 7. The rate of β3-tubulin positivity represented the neuronal differentiation rate. The rate of β3-tubulin positivity of the BMSCs supplemented with NSC-derived exosomes (6.344% ± 0.8251%, n =12) was higher than that of the BMSCs in basic culture medium (3.069% ± 0.886%, n = 10, P = .0138; Fig. 1C, D). Furthermore, the expression of neurofilament (NF), Map2, and β3-tubulin was significantly upregulated under NSC-derived exosome treatment (p_{NF} = 0.0009, p_{Map2} = 0.0033, $p_{\beta3\text{-tubulin}}$ = 0.028; Fig. 1E–H).

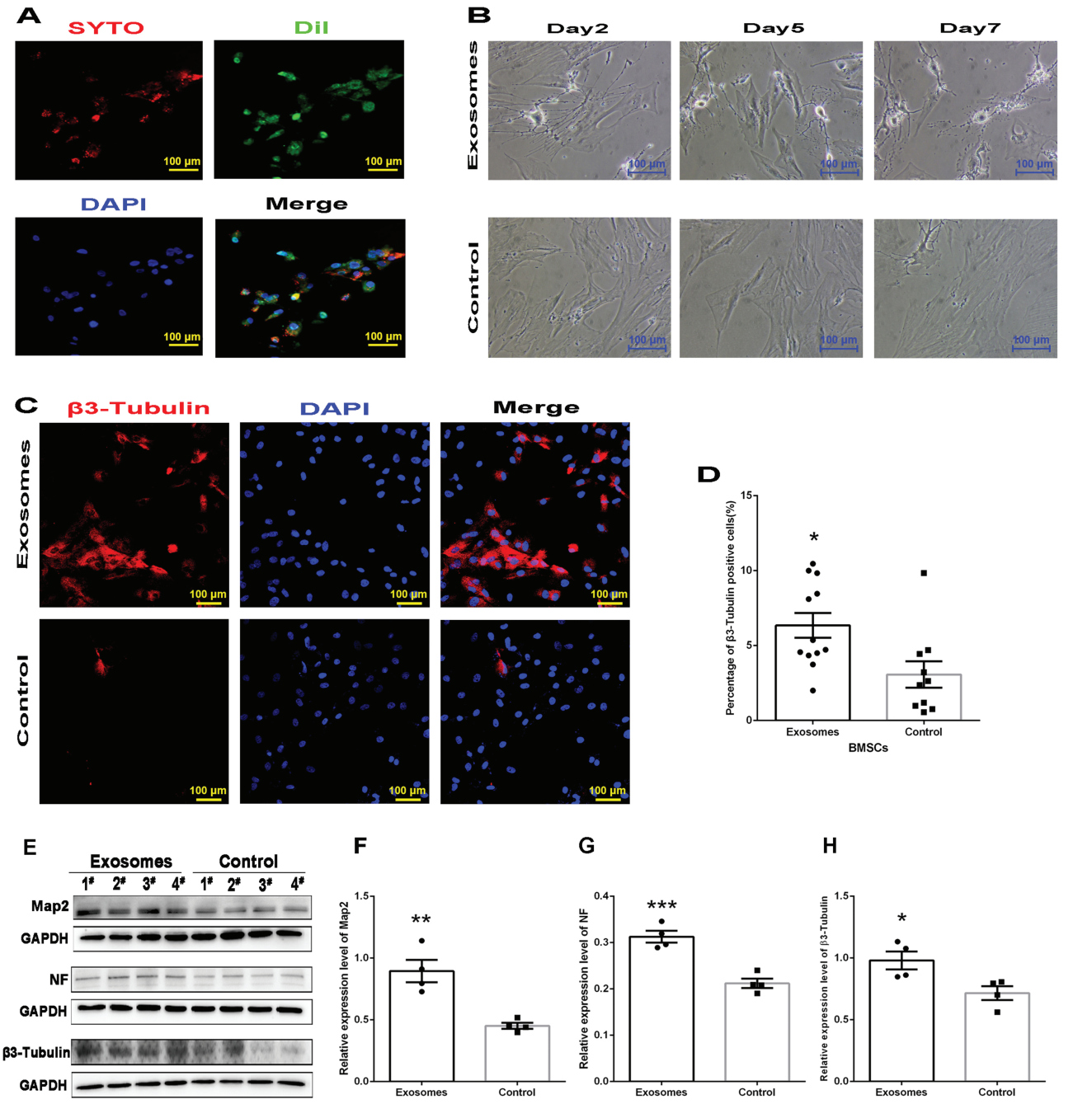

Figure 1. Neural stem cell (NSC)-derived exosomes promote bone marrow mesenchymal stem cell (BMSC) neuronal differentiation. (A) BMSCs were incubated with both Dio (green) and SYTO (red)-labeled exosomes for 24 h. BMSC nuclei were stained with DAPI (blue). Scale bar: 50 μm. (B) Morphological changes in BMSCs at days 2, 5, and 7. Scale bar: 100 μm. (C) Immunofluorescence staining of β3-tubulin. β3-tubulin (red) and DAPI (blue) staining are shown. Scale bar: 100 μm. (D) Histogram showing statistical analysis for the proportion of tubulin$^+$ cells, which was increased in the exosome-treated BMSC group compared with that in the control group. (E) Western blotting shows the relative expression of microtubule-associated protein (Map2), neurofilament (NF), and β3-tubulin in the NSC-derived exosome-treated BMSC and control groups. Histograms showing statistical analysis for the relative expression of Map2 (F), NF (G), and β3-tubulin (H). Relative protein levels of Map2, NF, and β3-tubulin were upregulated in the NSC-derived exosome-treated BMSC group compared with those in the control group. Four duplicate samples are shown (*: $P < .05$, **: $P < .01$, ***: $P < .001$).

To determine the ex vivo effect of NSC-derived exosomes in promoting BMSC neuronal differentiation, BMSCs supplemented with NSC-derived exosomes or left untreated were injected into the amniotic cavity of SBA embryos (Fig. 2A). The amniotic cavity was intact after amniocentesis, and all embryos presented neural tube closure defects before the injection was performed after 48 hours of ex vivo culture (Fig. 2B). The transplanted GFP-labeled BMSCs survived, migrated, and integrated into the defective spinal cord region (Fig. 2B, C). Frozen serial sections of the embryos were stained for β3-tubulin, synapsin-1, and GFP (Fig. 2D–G). The neuronal differentiation rate of BMSCs supplemented with NSC-derived exosomes was higher for β3-tubulin (BMSCs+Exosomes group: 52.09% ± 4.127%, BMSCs

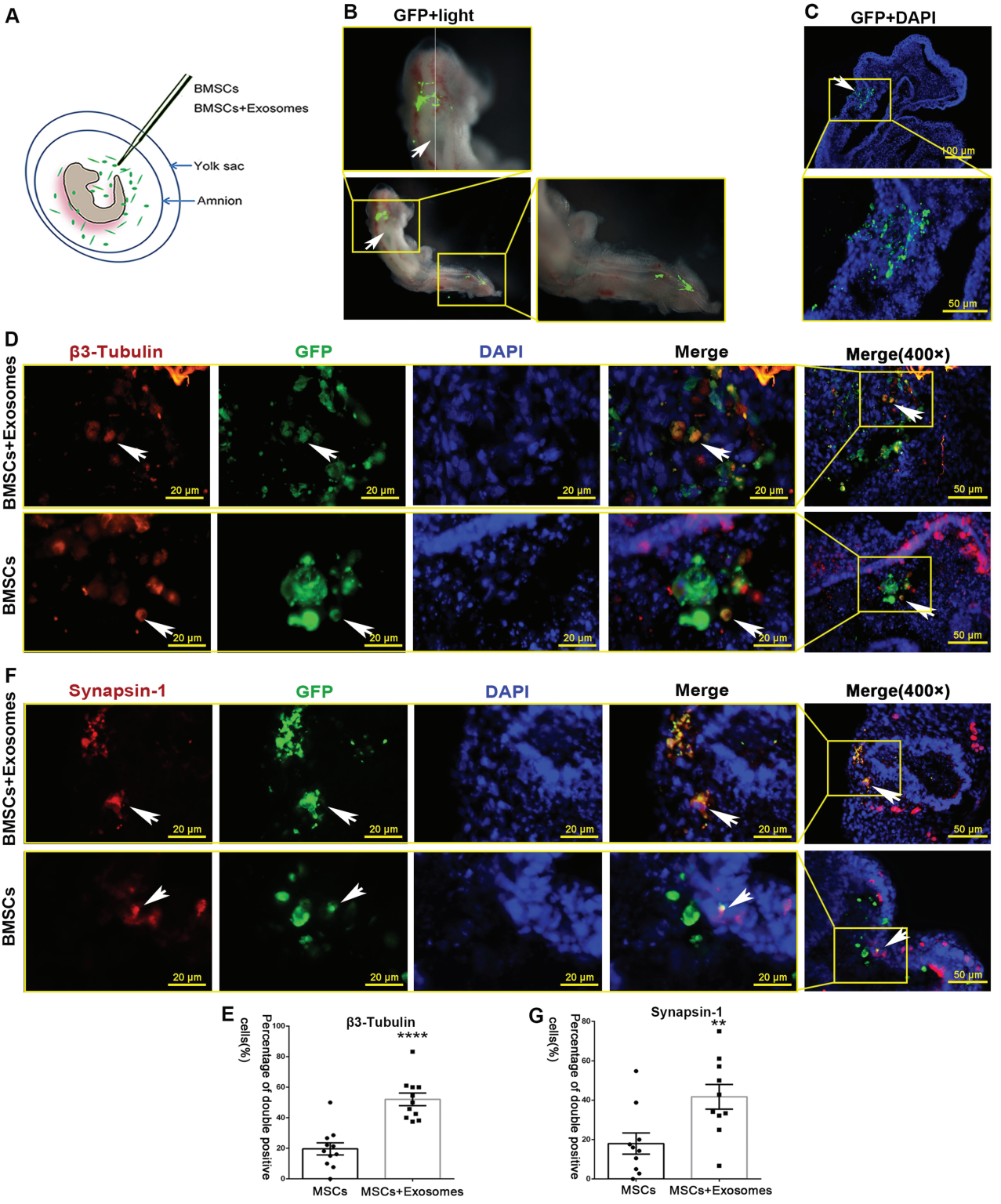

Figure 2. Neural stem cell (NSC)-derived exosomes promote neuronal bone marrow mesenchymal stem cell (BMSC) differentiation in ex vivo cultured embryos with spinal bifida aperta (SBA). (A) Pattern diagram of amniocentesis. Every embryo is shown to have an intact visceral yolk sac, and BMSCs with or without NSC-derived exosomes were injected into the amniotic cavity. (B) Embryos, cultured for 48 hours ex vivo, with developmental neural tube closure defects (arrow). Digitally enlarged images show BMSCs labeled with green fluorescent protein (GFP) (green) distributed specifically at defective region of neural tube. The vertical line in the enlarged image of the head of embryo represent that sections were made on the sagittal plane of SBA embryos. (C) Image of sagittal sections of embryo show that BMSCs labeled with GFP (green) integrated specifically into defective region of neural tube and survived (arrow). (D) Immunofluorescence staining for β3-tubulin (red) and GFP (green). Image and its digitally enlarged images show some of the neurons from the implanted BMSCs expressed β3-tubulin (arrow). (E) Histograms showing statistical analysis for the proportion of β3-tubulin$^+$ cells in transplanted BMSCs. (F) Immunofluorescence staining for synapsin-1 (red) and GFP (green). Image and its digitally enlarged images show some of the mature neurons differentiating from BMSCs expressed synapsin-1 (arrow). (G) Histograms showing statistical analysis for the proportion of synapsin-1$^+$ cells in transplanted BMSCs. (**: $P < .01$, ****: $P < .0001$).

group: 19.64% ± 3.951%, $P < .0001$, $n = 11$) and synapsin-1 (BMSCs+Exosomes group: 41.74% ± 6.253%, BMSCs group: 17.98% ± 5.363%, $P = .0099$, $n = 10$) than that of BMSCs cultured in normal medium (Fig. 2D–G).

Netrin1 Was Enriched in and Transported by NSC-Derived Exosomes

To identify proteins encapsulated in NSC-derived exosomes that could promote neuronal differentiation, we performed proteomic analyses on NSC-derived exosomes, NSCs, and BMSCs. NSC-derived exosomal proteins were annotated using GO terms. The top 20 enriched terms were considered, among which the terms "neuronal signal transduction" and "stem cell differentiation" indicated that the molecular function of NSC-derived exosomal proteins was mainly associated with neuronal differentiation (Supplementary Fig. S3). Thirty proteins were classified into the molecular function of positive regulation of neuronal differentiation (GO: 0045666). Next, the expression profiles of the 30 proteins were compared between NSC-derived exosomes and NSCs or BMSCs and are displayed as heat maps (Fig. 3A, B). Netrin1 (Ntn1), Nedd4l, Ptprz1, and Fn1 in NSC-derived exosomes showed higher expression than that in NSCs. In contrast, Pafah1b1, Camk2d, Gsk3b, Prpf19, Netrin1(NTN1), Rufy3, Camk2b, Ptprz1, and Reelin in NSC-derived exosomes showed higher expression than that in BMSCs. Moreover, after Coomassie Blue staining, SDS-PAGE showed a significantly enriched band located between 45 and 66.2 kDa on the lane for the NSC-derived exosomes, which was different from that for the NSCs and BMSCs (Fig. 3C). This finding indicated that NSC-derived exosomes can not only transfer but also enrich some proteins from their source cells. Netrin1 were further tested using Western blotting, it was confirmed to be enriched in NSC-derived exosomes and weakly expressed in BMSCs (Fig. 3D). Notably, the molecular weight of Netrin1, which is 64 kDa, is in the range of 45 to 66.2 kDa. Netrin1 expression in NSC-derived exosomes was higher than that in NSCs or BMSCs, similar to the expression of exosome marker, CD9 which was enriched in exosomes. GAPDH was used as a loading control (Fig. 3D).

Netrin1 Promoted BMSC and NSC Neuronal Differentiation In Vitro

Since the effect of Netrin1 on BMSC neuronal differentiation was unknown, we next investigated whether Netrin1 can promote neuronal differentiation of BMSCs and NSCs in vitro. First, we investigated the effect of Netrin1 on BMSC neuronal differentiation. After 12 days of BMSC culture in medium supplemented with 500 ng/mL exogenous soluble rNetrin1, the β3-tubulin-positive cell proportion (46.36% ± 3.295%, $n = 12$) significantly increased compared with that in untreated control BMSCs (14.98% ± 4.318%, $n = 9$, $P < .0001$) (Fig. 4A, B). Furthermore, the protein levels of Map2 ($P = .0001$), NF ($P = .0064$), and β3-tubulin ($P = .0061$) increased

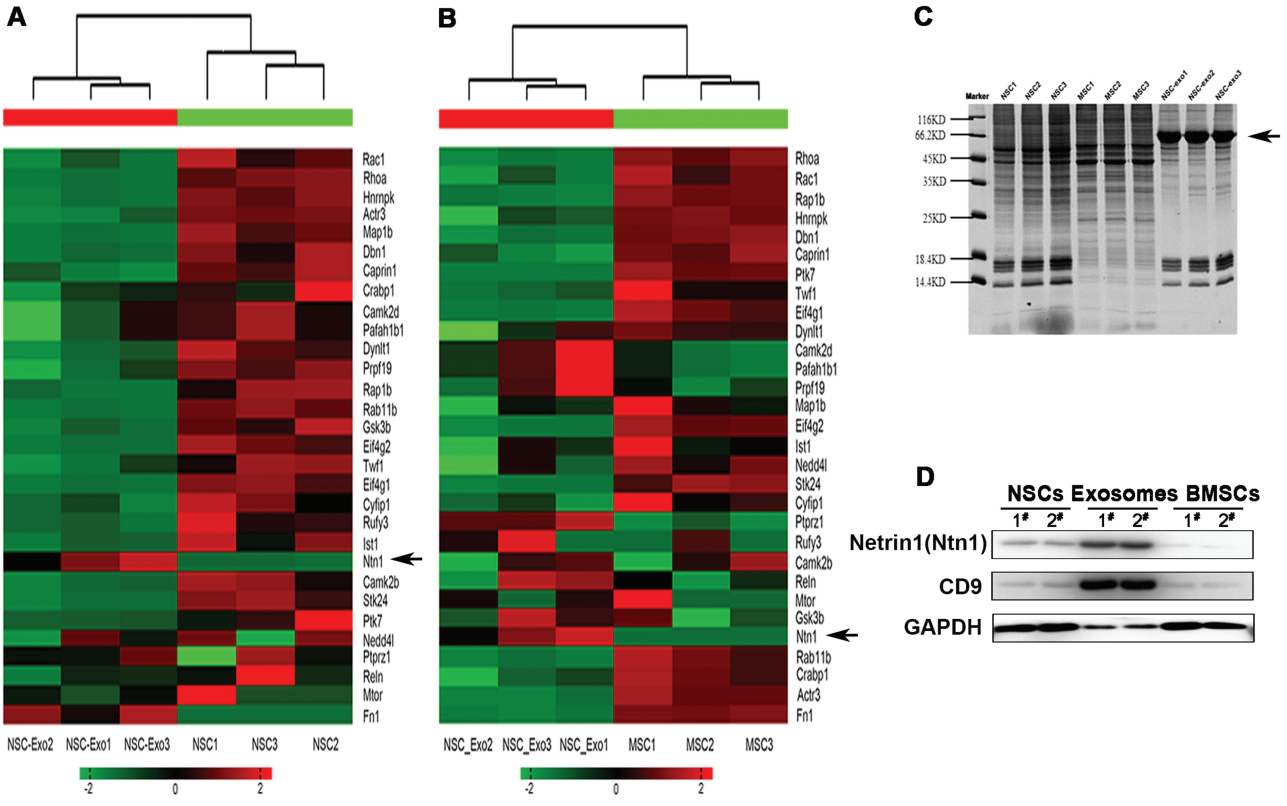

Figure 3. Exosomal proteins capable of promoting neuronal differentiation identified using proteomic analysis. (A) Heat map hierarchical clustering revealed 30 differentially expressed proteins in neural stem cell (NSC)-derived exosomes compared with those in the NSCs. (B) Heat map hierarchical clustering revealed 30 differentially expressed proteins in NSC-derived exosomes compared with those in bone marrow mesenchymal stem cells (BMSCs). Ntn1 (Netrin1) is indicated by an arrow. (C) Proteins were separated using sodium dodecyl sulfate-polyacrylamide gel electrophoresis. A high-density band was observed at 45-66.2 kDa in NSC-derived exosomes (arrow). (D) Expression levels of Netrin1 in NSCs, NSC-derived exosomes, and BMSCs.

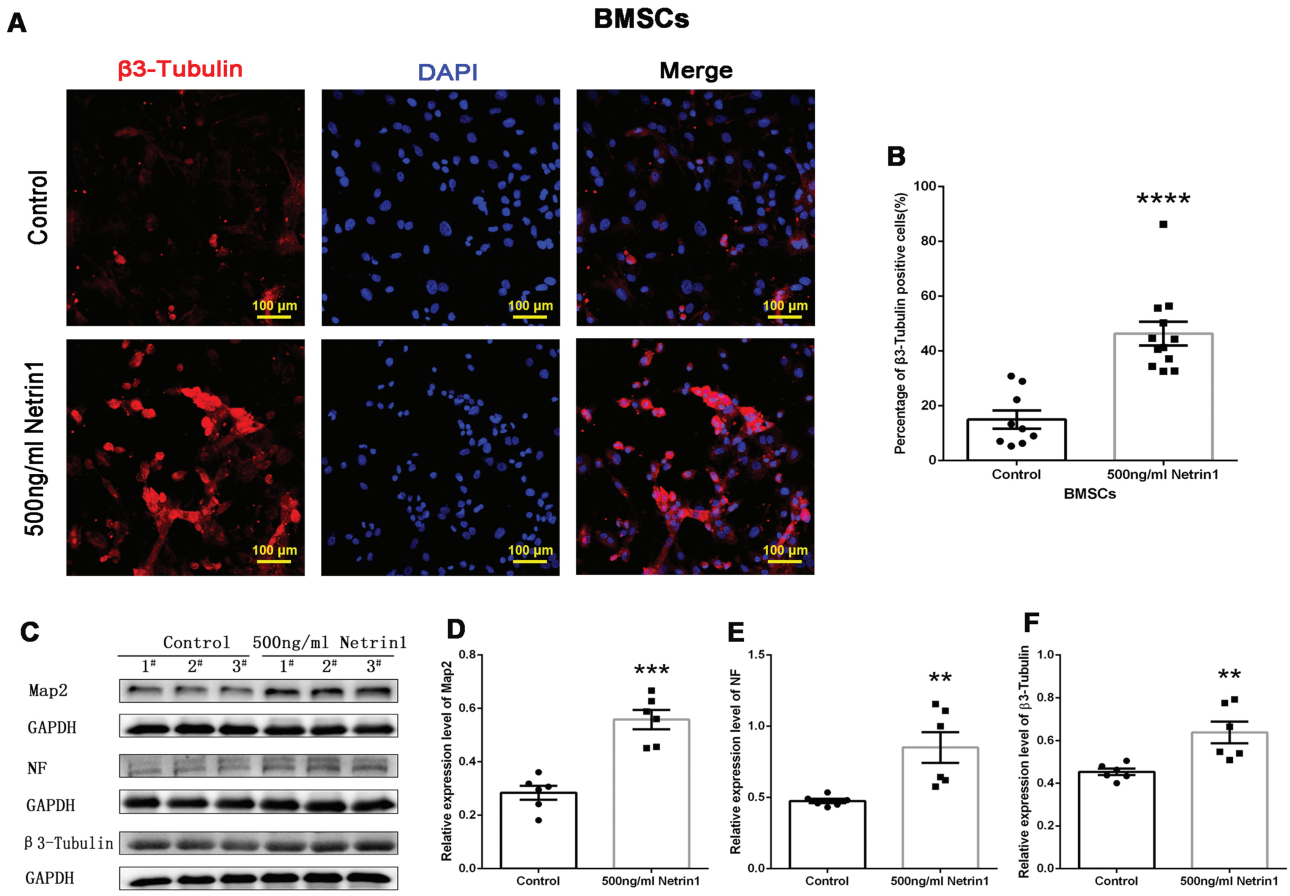

Figure 4. Netrin1 promotes the neuronal differentiation of BMSCs. (A) Immunofluorescence staining of β3-tubulin in BMSCs induced with 500 ng/mL recombinant Netrin1 (rNetrin1). β3-tubulin (red) and DAPI (blue) staining are shown as a counter stain. (B) Quantification of the proportion of β3-tubulin$^+$ cells. (C) Western blotting results showing the expression levels of Map2, NF, and β3-tubulin in 500 ng/mL rNetrin1-treated BMSCs. Histograms showing the statistical analysis for the relative expression of Map2 (D), NF (E), β3-tubulin (F). (**: $P < .01$; ***: $P < .001$; ****: $P < .0001$).

significantly in the Netrin1-treated BMSCs compared with those in untreated control BMSCs (Fig. 4C–F).

We further investigated the effect of Netrin1 on NSCs. After 7 days of NSC culture in medium supplemented with 500 ng/mL rNetrin1, the β3-tubulin-positive cell proportion (20.59% ± 1.624%, $n = 6$) significantly increased compared with those in control mouse NSCs (9.79% ± 0.8687%, $n = 6$, $P < .0001$; Fig. 5A, B). Furthermore, Western blot analysis showed a significant increase in Map2 ($P = .0068$), NF ($P = .0112$), and β3-tubulin ($P = .002$) levels in the Netrin1-treated mouse NSCs compared with those in control NSCs (Fig. 5C–F).

Netrin1 Promoted BMSC and NSC Neuronal Differentiation by Upregulating Hand2/Phox2b

To explore the mechanism underlying Netrin1-induced neuronal differentiation, a dataset (GSE54107) comprising RNA sequencing data of mouse fibroblasts and fibroblasts grown in media supplemented with rNetrin1 was downloaded from the GEO database. A total of 150 differentially expressed genes (DEGs) between the rNetrin1-treated and control groups were screened and integrated using the R software. A total of 76 up- and 74 downregulated DEGs were identified (Supplementary Table S1). To explore the proteins related with neuronal differentiation for the upregulated DEGs, the DAVID database was used to conduct GO analysis. Neural crest cell differentiation was found to be enriched in the biological process. Proteins for 3 upregulated DEGs (Hand2, Phox2b, and Wnt10a) were related to neural crest cell differentiation, whereas Hand2 and Phox2b were also related to sympathetic nervous system development (Fig. 6A). To better understand the interactions among the upregulated DEGs, the STRING online database was used to generate a PPI network. Interactions were observed between Hand2 and Phox2b (Fig. 6B), which suggested that Hand2/Phox2b are involved in Netrin1-induced neuronal differentiation.

Next, the expression of Hand2 and Phox2b was measured in NSCs and BMSCs treated with Netrin1. In both NSCs and BMSCs, we observed upregulated expression of Hand2 ($P = .0023$ and .0001, respectively) and Phox2b ($P = .0013$ and .0007, respectively; Fig. 6C–E) compared with that in untreated control cells (Fig. 6F–H).

Next, to explore whether the Hand2/Phox2b axis mediates Netrin1-induced neuronal differentiation, this signal axis was blocked using Phox2b knockdown. Phox2b shRNA3$^{\#}$ effectively downregulated the expression of Phox2b in NSCs (Fig. 7A, B) along with that of Map2, NF, and β3-tubulin (Phox2b shRNA3$^{\#}$ *vs* NC: $p_{\text{Map2}} = 0.0056$, $p_{\text{NF}} = 0.002$, $p_{\beta\text{3-tubulin}} < 0.0001$). Notably, Netrin1 upregulated the expression of Map2, NF, and β3-tubulin in NSCs transfected with NC shRNA, which was consistent with the result shown in Fig. 6C. However, Netrin1 did not upregulate the expression of Map2, NF, and β3-tubulin in NSCs with Phox2b

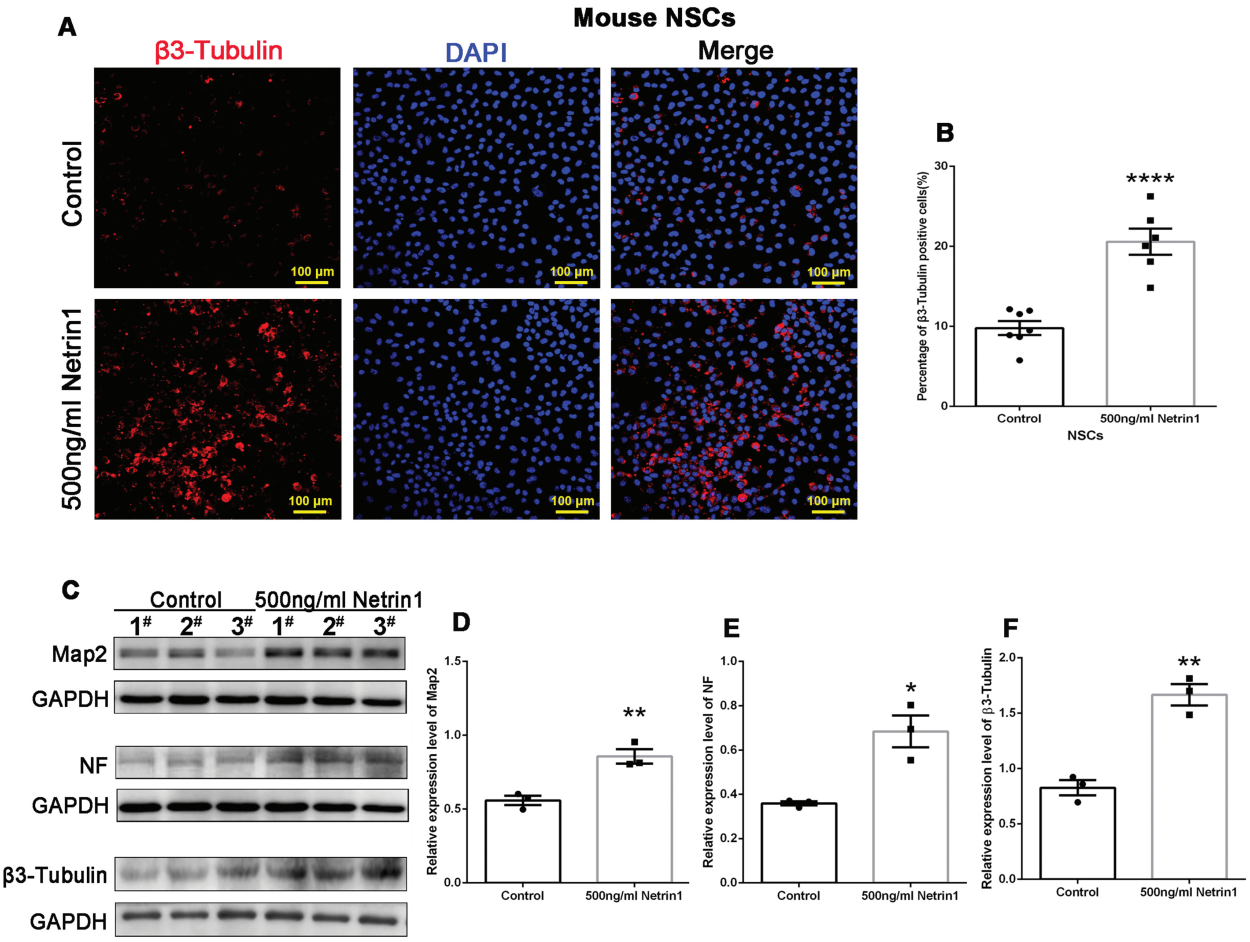

Figure 5. Netrin1 treatment promotes neuronal differentiation of neural stem cells (NSCs). (A) Immunofluorescence staining of β3-tubulin in the mouse NSC line induced with 500 ng/mL rNetrin1. β3-tubulin (red) and DAPI (blue) staining are shown as counter stains. (B) Quantification of the proportion of β3-tubulin$^+$ cells. (C) Western blots showing the expression levels of microtubule-associated protein (Map2), neurofilament (NF), and β3-tubulin in 500 ng/mL Netrin1-treated NSCs. Untreated NSCs served as the control. Histograms showing statistical analysis for the relative expression of Map2 (D), NF (E), β3-tubulin (F) (*: $P < .05$; **: $P < .01$; ****: $P < .0001$).

knockdown (Phox2b-RNAi + Netrin1 vs NC-RNAi + Netrin1: $p_{Map2} = 0.0001$, $p_{NF} = 0.0003$, $p_{\beta3\text{-tubulin}} = 0.0002$). Phox2b-RNAi blocked Netrin1-induced neuronal differentiation (Fig. 7C–F).

Discussion

Functional neuron deficiency in SBA is one possible reason for poor prognosis after surgical treatment. As neuron regeneration leads to better neural function recovery, we have been working on identifying methods to promote neuronal differentiation of transplanted BMSCs to improve neurological outcomes. Previous studies have shown that MSCs and NSCs exert positive effects on each other when co-cultured. On one hand, BMSCs are able to generate neural stem-like cells under neuronal differentiation induction of NSCs.[26] On the other hand, MSCs promote NSC proliferation and neuronal differentiation.[27] Furthermore, MSCs increase the survival rate of NSCs via regulating the microenvironment, induce neuronal development and neurite outgrowth, and improve transplantation outcome.[24,28,29] Recently, it has been shown that cells release numerous exosomes that can recapitulate the biological activity of the cells they are derived from. These exosomes are involved in cell-to-cell communication, cell signaling, and alteration of cell or tissue metabolism at short or long distances in the body. Exosomes can be used for cell-free regenerative medicine. Therefore, NSC-derived exosomes have emerged as a more promising treatment source than NSCs. Owing to their anti-inflammatory, neurogenic, and neurotrophic effects, NSC-derived exosomes are also useful for treating multiple neurodegenerative diseases.[30] Thus, in this study, NSC-derived exosomes were assessed as an excellent tool to improve neuronal differentiation of BMSCs. Combined NSC and MSC transplantation has an excellent therapeutic effect but is limited by host immune rejection and the source of NSCs used. We found that NSC-derived exosomes can replace NSCs, overcome the application limitations of NSCs, and achieve a good therapeutic effect. Exosomes have a higher safety profile than the cells themselves. Our research group has conducted a series of studies on the role of MSCs in the treatment of SBA. MSCs showed the ability of neuronal differentiation. The strategy of combined treatment with NSC-derived exosomes and BMSCs for SBA is novel, whereby the positive effects of both MSCs and exosomes are fully used.

Our in vitro experiments showed that NSC-derived exosomes promoted BMSC neuronal differentiation. Furthermore, NSC-derived exosomes benefited BMSC

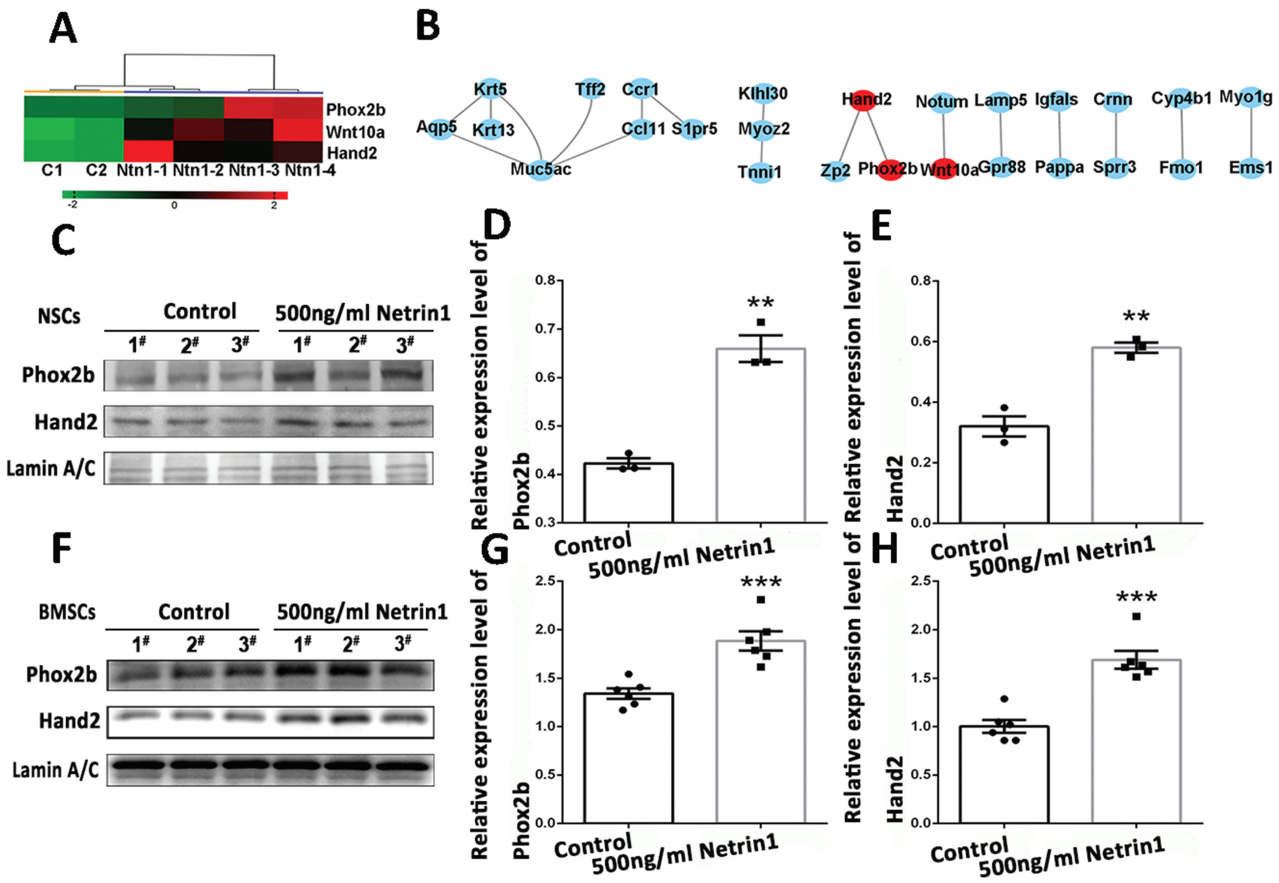

Figure 6. Mining functional proteins involved in Netrin1-induced neuronal differentiation via GEO and bioinformatic analyses, and verification of Phox2b and Hand2 expression induced by Netrin1 in BMSCs and NSCs, respectively. (A) Heat map of differentially expressed genes (DEGs) related to neural crest cell differentiation. (B) Protein–protein interaction network analysis of upregulated DEGs. (C) Western blots showing the expression levels of Hand2 and Phox2b in the 500 ng/mL rNetrin1-treated NSC group. Histograms showing statistical analysis for the relative expression of Phox2b (D) and Hand2 (E) in the 500 ng/mL rNetrin1-treated NSC and the control groups. (F) Expression levels of Hand2 and Phox2b in the 500 ng/mL rNetrin1-treated BMSC group. Histograms showing statistical analysis for the relative expression of Phox2b (G) and Hand2 (H) in the 500 ng/mL Netrin1-treated BMSC and control groups (*: $P < .05$; **: $P < .01$; ***: $P < .001$) .

therapy of rat embryos with SBA by directly promoting neuronal differentiation of the transplanted BMSCs. Considering that exosomes perform their functions via the biomolecules they encapsulate,[31-34] Netrin1 enriched and delivered by NSC-derived exosomes could be a major functional molecule that directs BMSC neuronal differentiation. Now-classic experiments characterized Netrin1 as an extracellular matrix (ECM) protein that guides axonal growth and cell migration during development.[35-37] We found that exosomes could play a role in intercellular communication by modulating ECM components. Exosomes can be considered among the structural and functional components of the ECM that participate in matrix organization and regulation of cells within the matrix, either directly or indirectly, via affecting matrix components.[38,39] Our study showed that NSC-derived exosomes provide a neural-specific ECM microenvironment through one of their cargo proteins Netrin1.

Functionally, Netrin1 exerts axonal attraction or repulsion and controls the guidance of CNS-conjugated and peripheral motor axons.[40] Netrin1 can induce neuronal differentiation in human embryonal carcinoma cells.[41] Conversely, Netrin1 can also regulate somatic cell reprogramming and pluripotency maintenance.[42] Therefore, the actual function of Netrin1 in inducing neuronal differentiation remains to be elucidated. In this study, we demonstrated that Netrin1 promotes neuronal NSC and BMSC differentiation. Notably, we previously demonstrated that the embryonic spinal cord niche is more conducive to MSC differentiation after transplantation.[16,43,44] The niche refers to the specific embryonic spinal cord environment that consists of multiple heterologous cell types and a niche-specific ECM. Here, we propose that Netrin1 is a functional molecule in the microenvironment of neural differentiation. Our in vitro data suggest that Netrin1 plays a role similar to that played by NSC-derived exosomes in inducing neuronal differentiation. Further studies are required to elucidate whether Netrin1 treatment on its own would elicit the same outcome as NSC-derived exosome treatment. Because the exosome is a vesicle containing a variety of bioactive molecules, and Netrin1 is one of functional proteins related to neuronal differentiation and high expressed in NSCs-derived exosomes, systematic testing is required to determine the optimal treatment dose.

Cell differentiation depends on sequential activation of transcription factors (TFs). In this study, our bioinformatic analysis predicted that Hand2 and Phox2b are downstream signal molecules. Hand2 belongs to the basic helix-loop-helix (bHLH) family of TFs for sympathetic neuron maintenance,[45,46] whereas Phox2b is a member of the paired family of

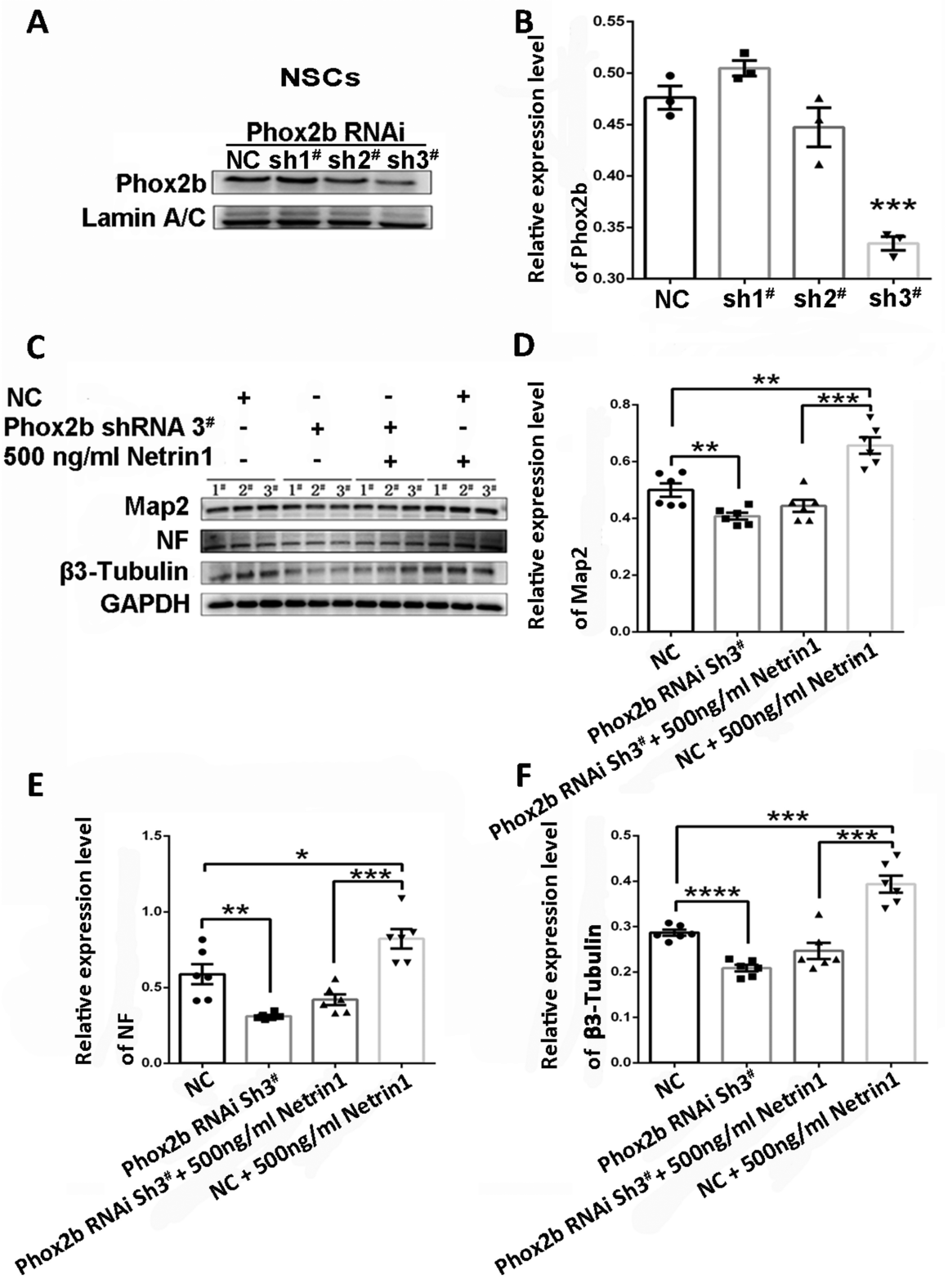

Figure 7. Netrin1 induces neuronal differentiation through the Hand2/Phox2b signal axis. (A) Knockdown efficiency of Phox2b in mouse neural stem cells (NSCs) evaluated via Western blotting. shRNA3# showed the most effective Phox2b knockdown. (B) Histograms showing statistical analysis for Phox2b expression in the 500 ng/mL Netrin1-treated BMSC and control groups. (C) Expression levels of the neuron markers microtubule-associated protein (Map2), neurofilament (NF), and β3-tubulin following Phox2b downregulation were measured in NSCs cultured with or without 500 ng/mL rNetrin1. Histograms showing statistical analysis for the relative expression of Map2 (D), NF (E), and β3-tubulin (F). (*: $P < .05$, **: $P < .01$, ***: $P < .001$, ****: $P < .0001$).

homeobox proteins. The balance between Phox2b and SOX10 determines the differentiation direction of neural cells. Phox2b promotes neuronal differentiation, whereas SOX10 promotes glial cell differentiation.[47] Moreover, the interaction of Hand2 with E2a is required for Phox2b transcription.[48] We found that Netrin1 treatment increased the levels of Hand2 and Phox2b in NSCs and BMSCs under neuronal differentiation, and the neuronal differentiation induced by Netrin1 depended on the upregulation of Phox2b. Hand2 and Phox2b are involved in the differentiation of noradrenergic neurons.[49] Furthermore, a recent study indicated that Hand2 and Phox2b, together with other 5 TFs (Ascl1, AP-2a, Gata3, Nurr1, and Phox2a), could convert astrocytes and fibroblasts into functional noradrenergic neurons.[50] Further studies should be conducted to determine the neuronal subtype that Netrin1 promotes BMSC or NSC differentiation to. Moreover, the mechanism underlying the upregulation of Hand2/Phox2b should also be elucidated in the future.

Conclusion

Although previous studies have provided knowledge regarding BMSC and/or NSC-based therapies for NTDs, the treatment effects have been disappointing. Here, we demonstrated that NSC-derived exosomes promote BMSC neuronal differentiation. Furthermore, we found that the mechanism underlying this effect involves exosome-mediated transfer of Netrin1, which upregulates Hand2/Phox2b nuclear TFs related to neuronal differentiation. The application value of NSC-derived exosomes was evaluated in BMSC therapy of SBA embryos. NSC-derived exosomes exerted the same therapeutic effects as NSCs, without the disadvantages associated with the use of NSCs. Thus, NSC-derived exosomes could replace NSCs. Our study, by providing novel insights into the role of exosomes and the ECM in neuronal differentiation, could facilitate the development of clinically useful exosomes. Given that the mechanism underlying neuronal direction of MSC differentiation induced by NSCs remains unclear, we focused on the role of NSC-derived exosomes, which are natural products of NSCs.

Funding

This work was supported by the National Key Research and Development Program (grant no. 2021YFC2701003, 2021YFC2701104), the National Natural Science Foundation of China (grant nos.: 82171649, 81871219), and the LiaoNing Revitalization Talents Program (grant no. XLYC1902099, XLYC1908008).

Conflict of Interest

The authors declared no potential conflicts of interest.

Author Contributions

L.M.: conception and design, collection and/or assembly of data, manuscript writing. X.W., W.M.: provision of study material or patients, data analysis and interpretation. Y.L., Y.W.: provision of study material or patients. Y.H., T.H.: administrative support. S.J., Y.W., W.L., D.L., and J.Y.: collection and/or assembly of data. H.G.: data analysis and interpretation. Y.B.: financial support. Z.Y.: conception and design, financial support, final approval of manuscript.

Data Availability

The data used to support the findings of this study are available from the corresponding author upon request.

Supplementary Material

Supplementary material is available at *Stem Cells Translational Medicine* online.

References

1. Lee S, Gleeson JG. Closing in on mechanisms of open neural tube defects. *Trends Neurosci*. 2020;43(7):519-532.
2. Pangilinan F, Molloy AM, Mills JL, et al. Replication and exploratory analysis of 24 candidate risk polymorphisms for neural tube defects. *BMC Med Genet*. 2014;15:102.
3. Moldenhauer JS. In utero repair of spina bifida. *Am J Perinatol*. 2014;31(7):595-604.
4. Dewan MC, Wellons JC. Fetal surgery for spina bifida. *J Neurosurg Pediatr*. 2019;24(2):105-114.
5. Buzhor E, Leshansky L, Blumenthal J, et al. Cell-based therapy approaches: the hope for incurable diseases. *Regen Med*. 2014;9(5):649-672. https://doi.org/10.2217/rme.14.35
6. Moll G, Ankrum JA, Kamhieh-Milz J, et al. Intravascular mesenchymal stromal/stem cell therapy product diversification: time for new clinical guidelines. *Trends Mol Med*. 2019;25(2):149-163. https://doi.org/10.1016/j.molmed.2018.12.006
7. Mahla RS. Stem cells applications in regenerative medicine and disease therapeutics. *Int J Cell Biol*. 2016;2016:6940283.
8. Zhao L, Chen S, Yang P, et al. The role of mesenchymal stem cells in hematopoietic stem cell transplantation: prevention and treatment of graft-versus-host disease. *Stem Cell Res Ther*. 2019;10(1):182. https://doi.org/10.1186/s13287-019-1287-9
9. Wang A, Brown EG, Lankford L, et al. Placental mesenchymal stromal cells rescue ambulation in ovine myelomeningocele. *Stem Cells Transl Med*. 2015;4(6):659-669. https://doi.org/10.5966/sctm.2014-0296
10. Shieh HF, Tracy SA, Hong CR, et al. Transamniotic stem cell therapy (TRASCET) in a rabbit model of spina bifida. *J Pediatr Surg*. 2019;54(2):293-296. https://doi.org/10.1016/j.jpedsurg.2018.10.086
11. Feng C, Graham CD, Connors JP, et al. A comparison between placental and amniotic mesenchymal stem cells for transamniotic stem cell therapy (TRASCET) in experimental spina bifida. *J Pediatr Surg*. 2016;51(6):1010-1013.
12. Wei X, Li H, Miao J, et al. Disturbed apoptosis and cell proliferation in developing neuroepithelium of lumbo-sacral neural tubes in retinoic acid-induced spina bifida aperta in rat. *Int J Dev Neurosci*. 2012;30(5):375-381. https://doi.org/10.1016/j.ijdevneu.2012.03.340
13. Li H, Gao F, Ma L, et al. Therapeutic potential of in utero mesenchymal stem cell (MSCs) transplantation in rat foetuses with spina bifida aperta. *J Cell Mol Med*. 2012;16(7):1606-1617. https://doi.org/10.1111/j.1582-4934.2011.01470.x
14. Li H, Miao J, Zhao G, et al. Different expression patterns of growth factors in rat fetuses with spina bifida aperta after in utero mesenchymal stromal cell transplantation. *Cytotherapy*. 2014;16(3):319-330. https://doi.org/10.1016/j.jcyt.2013.10.005
15. Li X, Yuan Z, Wei X, et al. Application potential of bone marrow mesenchymal stem cell (BMSCs) based tissue-engineering for spinal cord defect repair in rat fetuses with spina bifida aperta. *J Mater Sci Mater Med*. 2016;27(4):77. https://doi.org/10.1007/s10856-016-5684-7
16. Wei X, Cao S, Ma W, et al. Intra-amniotic delivery of CRMP4 siRNA Improves mesenchymal stem cell therapy in a rat spina bifida model. *Mol Ther Nucleic Acids*. 2020;20:502-517. https://doi.org/10.1016/j.omtn.2020.03.007

17. Cao S, Wei X, Li H, et al. Comparative study on the differentiation of mesenchymal stem cells between fetal and postnatal rat spinal cord niche. *Cell Transplant*. 2016;25(6):1115-1130. https://doi.org/10.3727/096368915x689910
18. Bai L, Lennon DP, Caplan AI, et al. Hepatocyte growth factor mediates mesenchymal stem cell–induced recovery in multiple sclerosis models. *Nat Neurosci*. 2012;15(6):862-870. https://doi.org/10.1038/nn.3109
19. Nakano R, Edamura K, Nakayama T, et al. Differentiation of canine bone marrow stromal cells into voltage- and glutamate-responsive neuron-like cells by basic fibroblast growth factor. *J Vet Med Sci*. 2015;77(1):27-35. https://doi.org/10.1292/jvms.14-0284
20. Song P, Han T, Xiang X, et al. The role of hepatocyte growth factor in mesenchymal stem cell-induced recovery in spinal cord injured rats. *Stem Cell Res Ther*. 2020;11(1):178.
21. Lescaudron L, Boyer C, Bonnamain V, et al. Assessing the potential clinical utility of transplantations of neural and mesenchymal stem cells for treating neurodegenerative diseases. *Methods Mol Biol*. 2012;879:147-164. https://doi.org/10.1007/978-1-61779-815-3_10
22. Sun L, Wang F, Chen H, et al. Co-transplantation of human umbilical cord mesenchymal stem cells and human neural stem cells improves the outcome in rats with spinal cord injury. *Cell Transplant*. 2019;28(7):893-906. https://doi.org/10.1177/0963689719844525
23. Dionigi B, Ahmed A, Brazzo J 3rd, Connors JP, Zurakowski D, Fauza DO. Partial or complete coverage of experimental spina bifida by simple intra-amniotic injection of concentrated amniotic mesenchymal stem cells. *J Pediatr Surg*. 2015;50(1):69-73.
24. Dionigi B, Brazzo JA 3rd, Ahmed A, et al. Trans-amniotic stem cell therapy (TRASCET) minimizes Chiari-II malformation in experimental spina bifida. *J Pediatr Surg*. 2015;50(6):1037-1041.
25. Shieh HF, Ahmed A, Rohrer L, et al. Donor mesenchymal stem cell linetics after transamniotic stem cell therapy (TRASCET) for experimental spina bifida. *J Pediatr Surg*. 2018;53(6):1134-1136. https://doi.org/10.1016/j.jpedsurg.2018.02.067
26. Croft AP, Przyborski SA. Generation of neuroprogenitor-like cells from adult mammalian bone marrow stromal cells in vitro. *Stem Cells Dev*. 2004;13(4):409-420.
27. Lee HC, Chang KC, Tsauo JY, et al. Effects of a multifactorial fall prevention program on fall incidence and physical function in community-dwelling older adults with risk of falls. *Arch Phys Med Rehabil*. 2013;94(4):606-615, 615.e1. https://doi.org/10.1016/j.apmr.2012.11.037
28. Park SE, Lee J, Chang EH, et al. Activin A secreted by human mesenchymal stem cells induces neuronal development and neurite outgrowth in an in vitro model of Alzheimer's disease: neurogenesis induced by MSCs via activin A. *Arch Pharm Res*. 2016;39(8):1171-1179. https://doi.org/10.1007/s12272-016-0799-4
29. Lee H, Kang JE, Lee JK, et al. Bone-marrow-derived mesenchymal stem cells promote proliferation and neuronal differentiation of Niemann-Pick type C mouse neural stem cells by upregulation and secretion of CCL2. *Hum Gene Ther*. 2013;24(7):655-669.
30. Vogel A, Upadhya R, Shetty AK. Neural stem cell derived extracellular vesicles: attributes and prospects for treating neurodegenerative disorders. *EBioMedicine*. 2018;38:273-282. https://doi.org/10.1016/j.ebiom.2018.11.026
31. Meldolesi J. Exosomes and ectosomes in intercellular communication. *Curr Biol*. 2018;28(8):R435-R444.
32. Mathivanan S, Ji H, Simpson RJ. Exosomes: extracellular organelles important in intercellular communication. *J Proteomics*. 2010;73(10):1907-1920.
33. Wang YY, Liu Q, Wang FC. Potential roles of exosome non-coding RNAs in cancer chemoresistance. *Oncol Rep*. 2020;45(2):439-447.
34. Skotland T, Sandvig K, Llorente A. Lipids in exosomes: current knowledge and the way forward. *Prog Lipid Res*. 2017;66:30-41. https://doi.org/10.1016/j.plipres.2017.03.001
35. Morales D. A new model for netrin1 in commissural axon guidance. *J Neurosci Res*. 2018;96(2):247-252.
36. Boyer NP, Gupton SL. Revisiting netrin-1: one who guides (axons). *Front Cell Neurosci*. 2018;12:221. https://doi.org/10.3389/fncel.2018.00221
37. Glasgow SD, Ruthazer ES, Kennedy TE. Guiding synaptic plasticity: novel roles for netrin-1 in synaptic plasticity and memory formation in the adult brain. *J Physiol*. 2021;599(2):493-505.
38. Rilla K, Mustonen AM, Arasu UT, et al. Extracellular vesicles are integral and functional components of the extracellular matrix. *Matrix Biol*. 2019;75-76:201-219.
39. Karamanos NK, Theocharis AD, Neill T, et al. Matrix modeling and remodeling: a biological interplay regulating tissue homeostasis and diseases. *Matrix Biol*. 2019;75-76:1-11.
40. Moore SW, Tessier-Lavigne M, Kennedy TE. Netrins and their receptors. *Adv Exp Med Biol*. 2007;621:17-31. https://doi.org/10.1007/978-0-387-76715-4_2
41. Mancino M, Esposito C, Watanabe K, et al. Neuronal guidance protein Netrin-1 induces differentiation in human embryonal carcinoma cells. *Cancer Res*. 2009;69(5):1717-1721. https://doi.org/10.1158/0008-5472.can-08-2985
42. Ozmadenci D, Féraud O, Markossian S, et al. Netrin-1 regulates somatic cell reprogramming and pluripotency maintenance. *Nat Commun*. 2015;6:7398. https://doi.org/10.1038/ncomms8398
43. Ma W, Wei X, Gu H, et al. Therapeutic potential of adenovirus-encoding brain-derived neurotrophic factor for spina bifida aperta by intra-amniotic delivery in a rat model.*Gene Ther*. 2020;27(12):567-578. https://doi.org/10.1038/s41434-020-0131-2
44. Xiaowei Wei, Wei Ma, Hui Gu, et al. Transamniotic mesenchymal stem cell therapy for neural tube defects preserves neural function through lesion-specific engraftment and regeneration. *Cell Death Dis*. 2020;11(7):523.
45. Rodrigues ACZ, Wang ZM, Messi ML, et al. Heart and neural crest derivative 2-induced preservation of sympathetic neurons attenuates sarcopenia with aging. *J Cachexia Sarcopenia Muscle*. 2020;12(1):91-108.
46. Stanzel S, Stubbusch J, Pataskar A, et al. Distinct roles of hand2 in developing and adult autonomic neurons. *Dev Neurobiol*. 2016;76(10):1111-1124. https://doi.org/10.1002/dneu.22378
47. Kim J, Lo L, Dormand E, et al. SOX10 maintains multipotency and inhibits neuronal differentiation of neural crest stem cells. *Neuron*. 2003;38(1):17-31. https://doi.org/10.1016/s0896-6273(03)00163-6
48. Hashimoto Y, Tsutsumi M, Myojin R, et al. Interaction of Hand2 and E2a is important for transcription of Phox2b in sympathetic nervous system neuron differentiation. *Biochem Biophys Res Commun*. 2011;408(1):38-44. https://doi.org/10.1016/j.bbrc.2011.03.113
49. Vincentz JW, VanDusen NJ, Fleming AB, et al. A Phox2- and Hand2-dependent Hand1 cis-regulatory element reveals a unique gene dosage requirement for Hand2 during sympathetic neurogenesis. *J Neurosci*. 2012;32(6):2110-20. https://doi.org/10.1523/JNEUROSCI.3584-11.2012
50. Li S, Shi Y, Yao X, et al. Conversion of astrocytes and fibroblasts into functional noradrenergic neurons. *Cell Rep*. 2019;28(3):682-697.e7. https://doi.org/10.1016/j.celrep.2019.06.042